SENSITIVITY STUDY OF VARIABLES ASSOCIATED WITH MAGNETIC RESONANCE IMAGING CAPILLARY PRESSURE MEASUREMENTS IN POROUS ROCKS

B.A. Baldwin[1], D. Green[2], J.C. Stevens[3] and J.J. Howard[3]

1 Green Country Petrophysics LLC, Dewey, OK, USA
2 Green Imaging Technologies, Fredericton, NB, Canada
3 ConocoPhillips, Bartlesville, OK USA

This paper was prepared for presentation at the International Symposium of the Society of Core Analysts held in Noordwijk, The Netherlands 27-30 September, 2009

ABSTRACT

Magnetic resonance imaging of centrifuged core plugs provides a unique method for the rapid determination of capillary pressure curves in porous rocks. The technique is based on the concept that properly collected images show the actual distribution of fluid(s), at a high spatial resolution, along the entire length of the core sample. The calibrated images provide high resolution saturation information that is matched with capillary forces generated along the length of the core during centrifugation. This method is dependent upon the centrifuge procedures used to generate the distribution of fluids in the core and the MRI data acquisition techniques. Fluid distributions are sensitive to a number of procedural variables associated with the measurement including the location of the core plug's base (Pc=0), centrifuge speed, length of centrifuging time, rate of fluid(s) redistribution following centrifugation, and the effect of heterogeneity in the plug. Footbaths were found to be a valuable aid for maintaining 100% saturation at the outlet end in order to define the Pc=0 point. The location of the actual core plug outlet in the MRI image is affected by rock type, which in turn influences the capillary pressure calculations.

INTRODUCTION

Soon after the introduction of magnetic resonance imaging technology, MRI, it was recognized that this non-destructive, non-invasive technique could provide saturation data for capillary pressure curves [1, 2]. This study looks at the sensitivity of several variables involved with collecting MRI measurements on saturated and centrifuged core plugs in a water/air system. The objective was to determine the most critical aspects of the technique and offer suggests for improvements. Previous studies have demonstrated the connection between MRI-generated saturations distributions and capillary pressure curves [1, 3], so the objective of this study was to determine the most critical aspects of the technique and the role of a footbath in establishing uniform and consistent boundary conditions.

There are several well established centrifuge-based methods for determining capillary pressure information from core plugs [4–6]. All involve the displacement of a fractional volume of liquid, usually water, from a core while spinning at high speeds in a centrifuge. Changes in the spin speed alter the pressure range. A key assumption in

many of these centrifuge experiments is that at a known point in the core the boundary condition of zero capillary pressure is met [7]. MRI images of a centrifuged core provide direct evidence of the distribution of fluids in the core and whether the Pc=0 boundary condition is satisfied. These images also allow one to determine the effectiveness of using footbaths in the centrifuge experiment to establish the zero pressure boundary condition. The role of a footbath in a centrifuge experiment is to define precisely the position where the boundary condition Pc=0 is located, though there remains some uncertainty over the effectiveness of many footbath designs [2, 5, 6].

For this particular study we focused on duplicate Berea plugs at two permeabilities. Other types of rock are expected to exhibit different responses and need to be examined.

EXPERIMENTAL

All magnetic resonance images, MRI, were obtained with a Unity/Inova-Imaging 85/310 spectrometer (Varian Inc., Palo Alto, CA) operated at a resonance of 85.7098 MHz, 2T, to measure hydrogen. The RF coil was a 13.3 cm (5.25") ID 85 MHz ^{1}H Quadrature Bird Cage Coil with an RF window 27.9 cm (11.0") long. It consisted of 16 low-pass elements separated into two channels with independent tuning and matching. The tuning range was 2.7 MHz and unloaded Q was 520. A spin-echo pulse sequence was used to obtain images with a resolution of 0.47 x 0.50 mm.

The schematic drawing of the capillary pressure cell used in this work and pertinent centrifuge dimensions are shown in Figure 1. The cell was constructed from nylon with an o-ring seal in the lid to minimize fluid evaporation while centrifuging and collecting MRI images. The water expelled from the core remained in the cell, but below the core and image when it was oriented horizontally in the MRI. This minimized the handling of the plug and exposure to the atmosphere where evaporation would occur. The housing and top were marked so that the cell could be placed in the same orientation in the centrifuge and MRI for multiple experiments. This orientation, and a little care, prevented expelled water from contacting the core and possibly imbibing back into it. The plug sat on a 2.54 cm tall nylon spacer to prevent the expelled water from re-contacting the plug. The vertical bars connected to the cap contained nylon screws, which were used to center the plug in the cell and prevented movement while centrifuging, transporting and collecting MRI images.

The capillary forces generated by centrifuging were determined by

$$Pc = \frac{1.588 * 10^{-7} \Delta\rho\left(r_{out}^2 - r_x^2\right) rpm^2}{2} \qquad (1)$$

Where Pc is in psi, r_{out} is the radius (cm) at Pc=0 i.e. r_{base} minus the footbath depth, r_x is the radius (cm) corresponding to the individual MRI voxel locations, rpm is the rotating speed in revolutions per minute and $\Delta\rho$ is the density difference (g/cm^3) between the fluids saturating the core plug. The units in constant were chosen so that Pc was determined in psi, a unit commonly used in reservoir engineering and simulation.

To assure 100% saturation at the bottom of the plug while centrifuging several footbaths were tested. The footbath depth ranged from 0.0 to 1.0 cm.

The footbaths were constructed to minimize the amount of water available for imbibition back into the core when the centrifuge was stopped.

Centrifuging was performed in a Sorvall RC 6 Plus using the HS4 horizontal swing head. Speed was set and controlled by the unit. The orientation and pertinent dimensions of the cell and sample are given in Figure 1.

Four Berea sandstone plugs were selected for preliminary experimentation Table 1. Two had higher permeability, ~800 mD and two lower permeability, ~200 mD. The plugs were saturation with 0.1 wt % NaCl. This low value was used to minimize clay effects and yet allow the plugs to be simply dried before the next saturation rather than cleaned with methanol.

All of the experiments reported here produced drainage curves using brine and air as the two phases. A typical experiment consisted of saturating the core with brine, collecting a base-line image at 100% saturation with the plug in the cell, centrifuging he plug in the cell for a pre-determined time and speed, removing the cell and plug from the centrifuge, placing the cell and plug into the MRI and begin imaging within less than three minutes after stopping the centrifuge. MRI imaging collects most the intensity information half-way through the total scan time. Thus, the intensity reported here was collected within as short as ca. 7 min to as long as several hours after stopping the centrifuge.

RESULTS AND DISCUSSION

Figure 2 shows a representative image of 100% brine saturated Berea 501. The spot to the left is plug of silicon sealant embedded in the cell base as a check of positioning. Capillary pressure measurements can be obtained quicker by only collecting profiles of the sample, but for this sensitivity study we measured multiple 2D images to also ascertain the homogeneity of the water distribution. The MRI intensity averaged across one plug (Berea 501) for seven independent water saturations and MRI measurements are shown in Figure 3. Reproducibility between 7 images collected over 8 days was very good with the average standard deviation between the seven plots being 2.7% of the average value. The structure observed in the curves is not random, but represents the bedding planes, which are seen as vertical stripes in Figure 2. To achieve this level of reproducibility the plug was dried, subjected to a vacuum until a pressure of ca. 110 millitorr was achieved and saturated with thoroughly de-gassed brine. With our system it took approximately an hour at 110 millitorr to thoroughly de-gas our brine. The sample cell, containing the core plug, was re-positioned within less than 1 mm between independent measurements using a tray and horizontal stops. This assured that the sample was in the same location relative to the magnet center for each measurement.

Figure 4 shows a comparison of representative average MRI intensity along the centrifugal axis for all four samples at 100% brine saturation. Although there is good agreement between the two plugs at each permeability, there is a significant difference in MRI intensity that cannot be explained solely by the different porosity of the two samples. If the only difference between the two samples was the amount of water in the plug the 100 series plugs should have a MRI intensity of 0.0102 when the 500 series plugs averaged 0.0126. The 100 series plugs showed an average MRI intensity of

0.00302, significantly lower than expected from porosity alone. This suggested that the lower permeability plugs contained some magnetic or para-magnetic component(s) that reduced the T_2^* relaxation time below the ability to quantitatively collect the intensity with spin-echo imaging.

The reproducibility of producing a centrifuged brine distribution is show in Figure 5 for three independent preparations and measurements of Berea plug 501 after > 10 hrs of centrifuging at 750 rpm. This process included saturation, centrifugation and MRI measurement. The reproducibility between the three experiments was very good with the average standard deviation being 2.1%. Again accurate re-positioning of the sample in its cell was vital. (removed two sentences in the middle re: earlier images)

Figure 6 shows the effect of improper sample preparation where three examples are compared to a properly prepared sample. In an attempt to speed up the process the plugs were not dried for these three tests. Rather the previously centrifuged plug was placed directly into the vacuum chamber and subjected to a vacuum for less than an hour and the water de-gassed for less than ten minutes. The reproducibility of images and weights of the 100% re- saturated plugs appeared to be in the normal range, but the three centrifuged samples all showed excessive brine in the transition and residual zones (2 – 6 cm). However, the threshold saturations (1.7 cm) are comparable for all four samples. Based on prior, unreported experience, it was suspected that these humps represent trapped air and loss of connected water paths to properly drain the sample. Including them would significantly shift the resultant capillary pressure curve.

The effect of the footbath depth on the distribution produced while centrifuging brine at 750 rpm is shown in Figure 7 for 0.0, 0.5 and 1.0 cm. In Figure 8 the distributions are aligned to the top of the respective footbath, Pc=0. The brine saturation distributions in the transition and residual zones are slightly different because these images do not take into account pressure differences imposed by the height of the plug's top above the footbath top. The two experiments with footbaths have ca. 100% saturation at Pc=0 while the sample with 0.0 cm footbath has a similar threshold saturation, but is less than 100% brine saturated at the base of the plug. The latter, 100% saturation at Pc=0 is the basic assumption of centrifuge methods for determining capillary pressure.

The effect of the footbath on saturation at the outlet of the plug becomes more pronounced with increasing speed. Figure 9 shows brine saturation distributions for 0.0 and 1.0 cm footbaths after 750, 1000 and 1500 rpm experiments. The 1.0 cm footbath results in substantial brine saturation above the footbath while the 0.0 footbath resulted in a significantly reduced saturation at the bottom of the plug. With the footbath the brine saturation decreased with increasing speed, but ca. 100% saturation was achieved near or above the top of the footbath, solid black line. With no footbath all the plugs were all less than 100% saturation, at the bottom of the plug, dashed black line. However, they did exhibit higher saturations at the very bottom of the plug compared to the top. All of these experiments were centrifuged for 31 minutes to minimize the effect of thin film drainage on the surface of the nylon, non-water wetting footbath. These results suggested that another mechanism was causing the plugs to de-saturation more than expected from capillary pressure considerations alone.

Redistribution of the brine following centrifuging can effect the capillary pressure calculation if it occurred while the distribution was being measured. It was found that the rate of redistribution was dependent on the rock and footbath used. Figure 10 shows the distribution as a function of time after centrifuging for Berea 502. During this redistribution the total average intensity was constant corroborating re-distribution rather than evaporation or other loss of water. The lower permeability Berea showed a much lower rate of redistribution, not shown, and a North Sea chalk sample, <10 mD permeability and much smaller pores < 1 um vs ~100 um for Berea, exhibited only 1-2 % re-distribution over a 494 day period of observation, not shown.

For the calculation of Pc by Equation 1 knowing the actual bottom of the core is important. Because some rock materials cause a broadening of the NMR spectrum they can obscure the accurate location of the end of the sample. A simple holder was constructed that allowed alignment and simultaneous imaging of the end of the sample and a phantom filled with brine. The MRI intensity at one end is shown in Figure 11 for Berea 501, a chalk plug and the phantom. For the phantom the intensity dropped from its maximum value to background within no more than one intermediary point. This point represents a voxel partially filled with brine at the edge. The chalk sample, which contained few magnetic materials, exhibited a similar change. However, the Berea plug had about an 8 point range (ca. 4 mm) from the intensity in the plug interior to baseline. The true end of the plug was halfway between the maximum intensity and background. The importance of knowing the location of the plug base is shown by the two capillary pressure curves shown in Figure 12. In one case the apparent end of the plug was assumed with the first drop in MRI intensity and in the other the location was determined by comparison with the phantom above. Although the base location shifted only 2 mm, the difference in threshold pressure, point where drainage begins, and the transition zone, between Sw = 1 and about 0.3, was significant, about 10%. The residual value, Swf, was unchanged because it is unaffected by the plug position.

The experiments described above are the first step for examining how best to use the high resolution of MRI and centrifuge techniques to more rapidly and accurately obtain capillary pressure curves. Other variables that need to be examined include the length of the centrifuge time, NMR/MRI pulse sequences that minimize the effect of relaxation producing images that more accurately reflect the amount of water present without calibration and other rock types.

CONCLUSIONS

- Repeatability of the total process including sample preparation, centrifuging and MRI image acquisition was very good.
- Sample preparation was critical to acquiring good results
- Re-distribution of fluids can be a problem for determining saturation distribution in some samples
- Footbaths provide 100% saturation at the sample outlet
- Accurate identification of the sample base is important for good capillary pressure curves

REFERENCES

1. Baldwin, B.A., and Yamanashi, W.S., Sept.-Oct. 1991, "Capillary-Pressure determinations from NMR Images of Centrifuged Core Plugs: Berea Sandstone", *The Log Analyst,* pp. 550-556.

2. Baldwin, B.A., and Spinler, E.A., 1998, "A direct method for simultaneously determining positive and negative capillary pressure curves in reservoir rock", *J. Pet. Sci. Eng.* v. 20, pp 161-165.

3. Green, D.P., Dick, J.R., Gardner, J., Balcom, B.J., and Zhou, B., "Comparison study of capillary pressure curves obtained using traditional centrifuge and magnetic resonance imaging techniques", SCA2007-30.

4. Christiansen, R.L., 2008, *Multiphase Flow Through Porous Media*, KNQ Engineering, Salt Lake City, UT.

5. Al-Omair, O. A., 2009, "New experimental method for measuring drainage and spontaneous imbibition capillary pressure", *Energy & Fuels*, v. 23, pp. 260-271.

6. Ruth, D.W., and Chen, Z.A., 1995, "Measurement and interpretation of centrifuge capillary pressure curves – the SCA survey data", *Log Analyst*, v. 36, no. 5, pp. 21-32.

7. O'Meara, D.J., Hirasaki, G.J., and Rohan, J.A., 1992, "Centrifuge measurements of capillary pressure: Part 1 – Outflow boundary condition", *SPE Res. Eng.*, v. 7, pp. 133-142.

Table 1
Properties of Berea Sandstone Samples

Sample	Length cm	Diameter cm	Pore Volume ml	Porosity %	Permeability mD
101	**6.44**	**2.53**	**5.940**	**18.36**	**179.2**
102	**6.50**	**2.53**	**5.985**	**18.35**	**168.3**
501*	**6.60**	**2.53**	**7.461**	**22.65**	**807.4**
502	**6.52**	**2.53**	**7.361**	**22.62**	**802.5**
*** after break**	**5.52**	**2.53**			

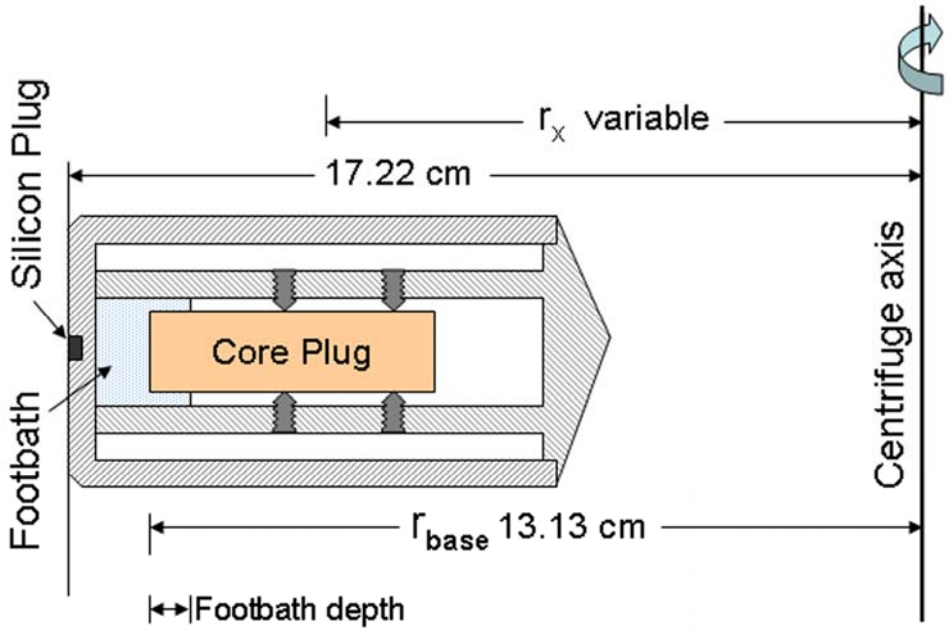

Figure 1 Schematic cross sectional drawing of MRI capillary pressure cell and dimensions needed for capillary pressure calculations.

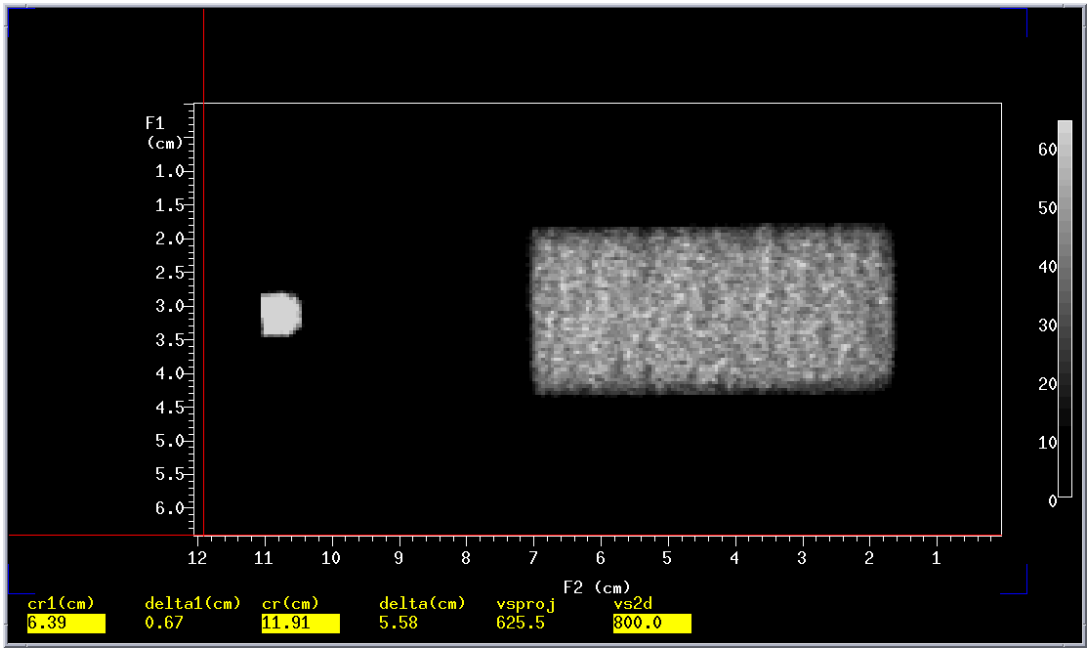

Figure 2 MRI image of 100% brine saturated Berea plug 501 with reference silicon RTV plug in base of cell to the left.

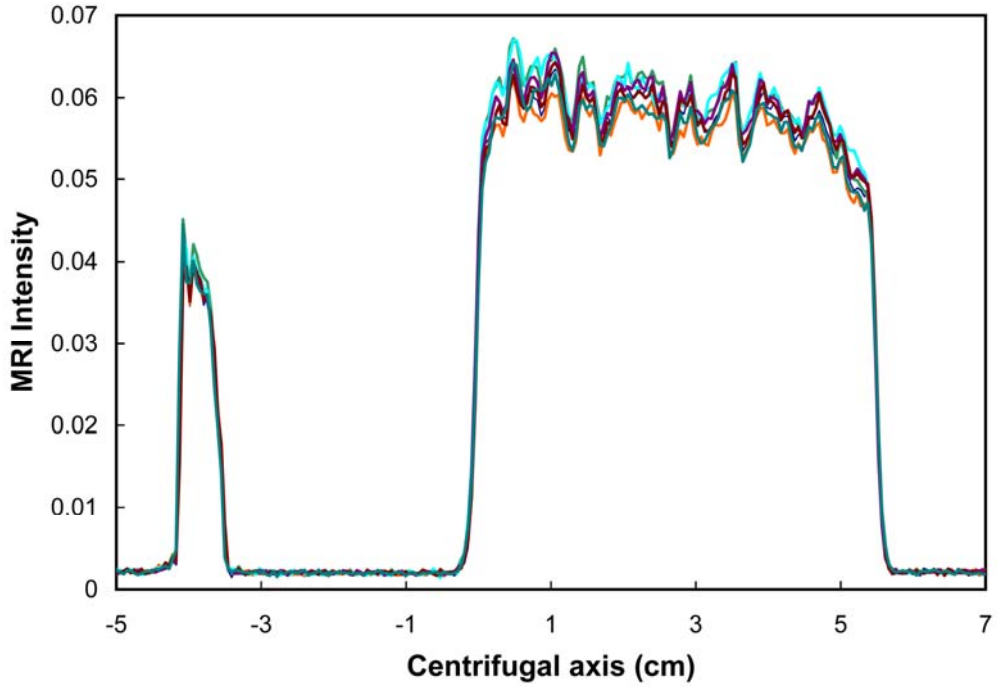

Figure 3 MRI intensity distributions for seven independent saturations and measurements of Berea plug 501 at 100% brine saturation.

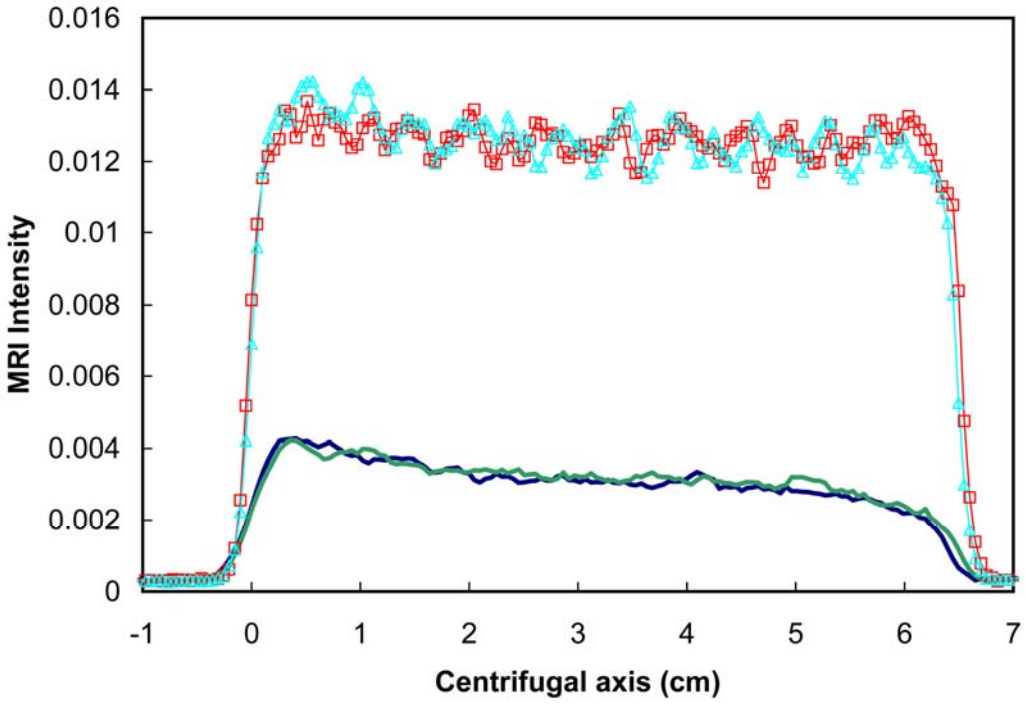

Figure 4 MRI intensity distributions at 100% saturation for four Berea plugs □ 501, Δ 502, – 101, – 102.

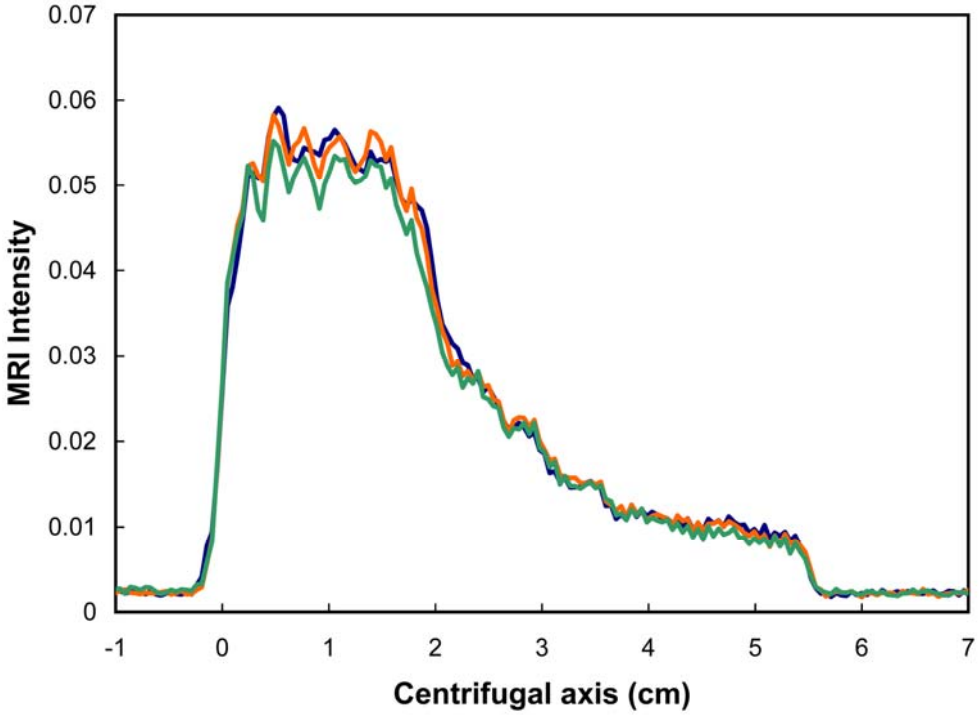

Figure 5 MRI intensity distribution after centrifuging at 750 rpm for three independent experiments on Berea 501.

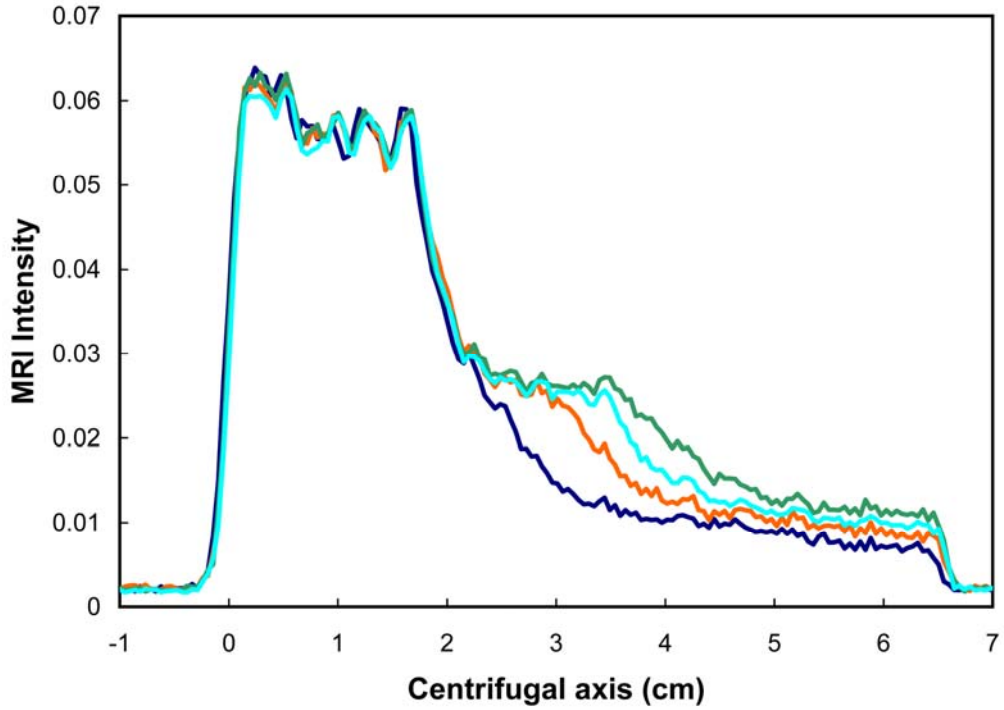

Figure 6 MRI intensity distribution after centrifuging at 750 rpm for one properly and three improperly prepared experiments on Berea 501.

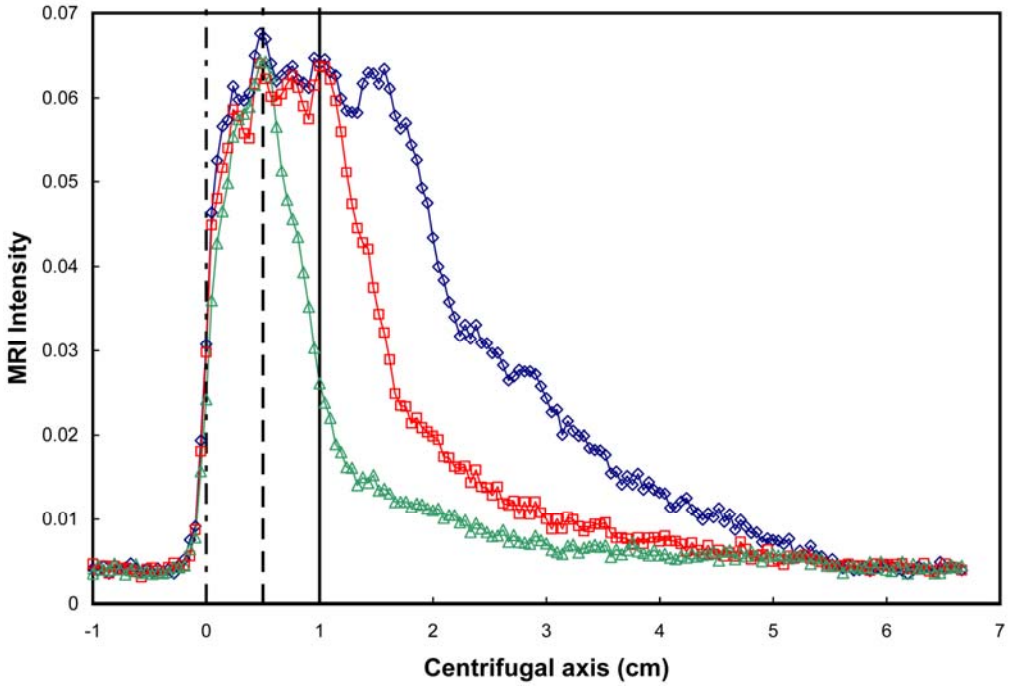

Figure 7 MRI intensity distributions after centrifuging Berea 501 at 750 rpm with three footbath depths Δ 0.0 cm, □ 0.5 cm, ◊ 1.0 cm, vertical lines are top of footbath at - - - 0.5 cm and 1.0 cm.

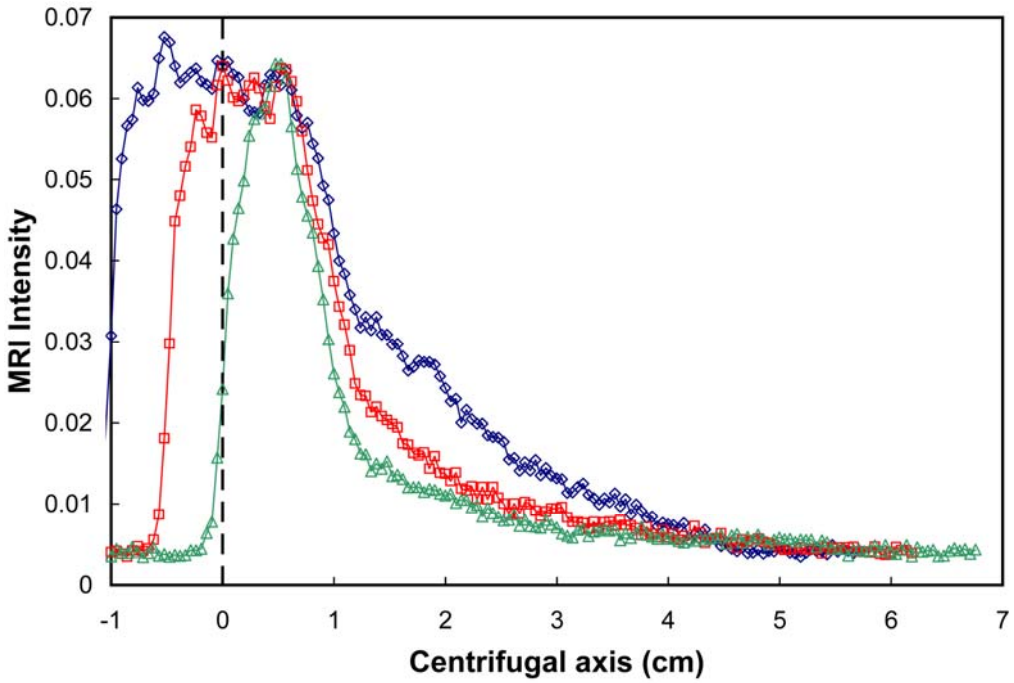

Figure 8 MRI intensity distribution curves in Figure 7 with three footbath depths, Δ 0.0 cm, □ 0.5 cm, ◊ 1.0 cm, shifted so that 0 cm is the top of the footbath where Pc = 0.

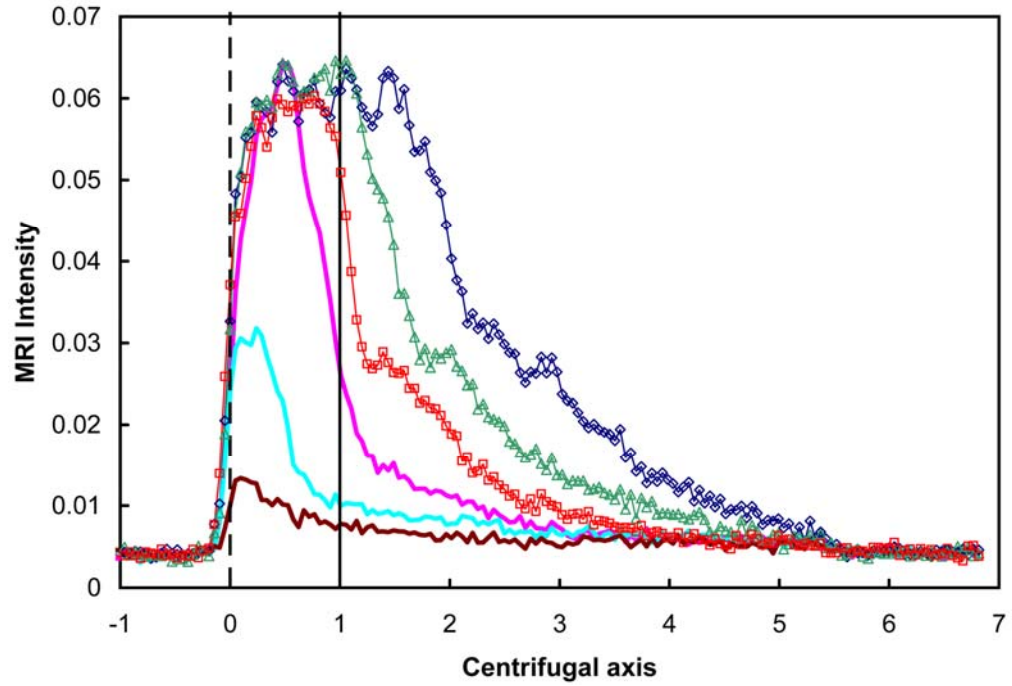

Figure 9 MRI intensity distributions after centrifuging Berea 501 at three speeds with and without a 1 cm footbath 750 rpm – 0.0 cm, ◊ 1.0 cm, 1000 rpm – 0.0 cm, Δ 1.0 cm, 1500 rpm – 0.0 cm, □ 1.0 cm.

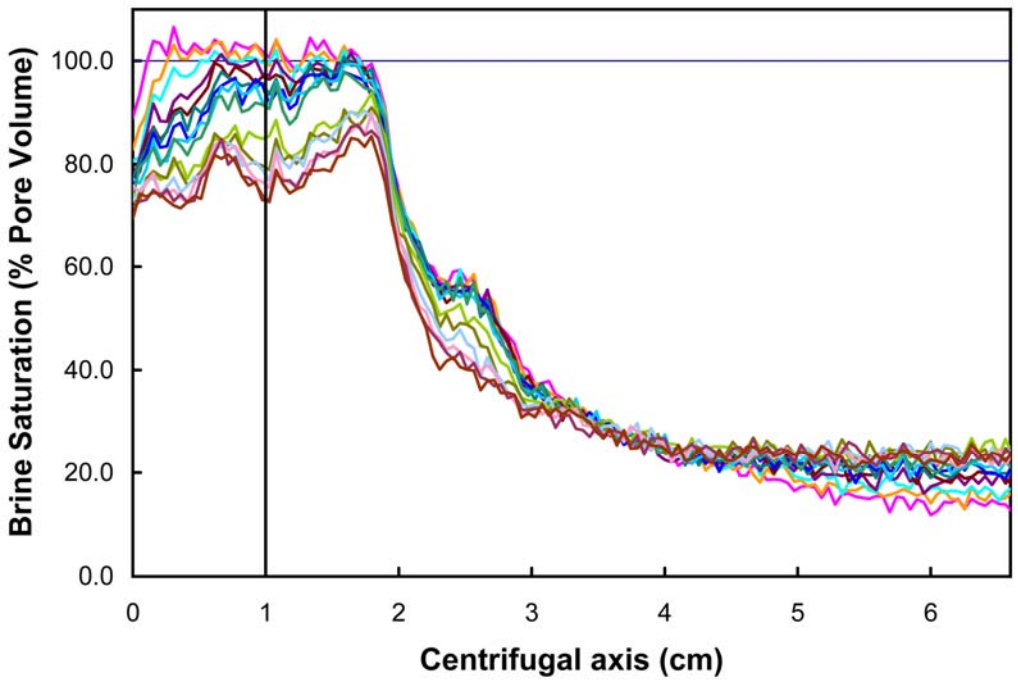

Figure 10 Brine saturation as a function of time following centrifuging Berea 502 at 750 rpm decreasing saturation on left and increasing saturation on right

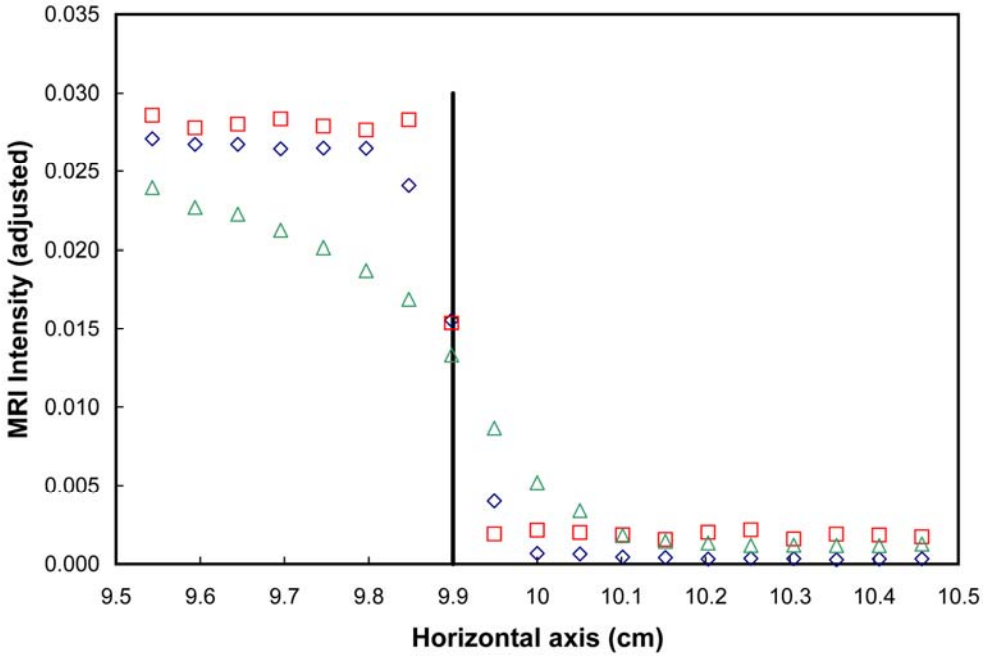

Figure 11 Comparison of end effects on MRI intensity for three samples ◊ brine in phantom, □ brine in chalk, Δ brine in Berea sandstone, intensities adjusted to provide comparison, line is base of samples

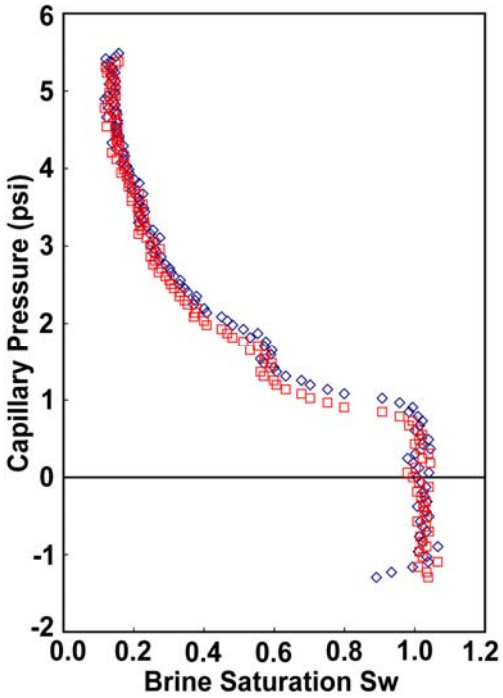

Figure 12 Effect of the location of the plug base on capillary pressure calculation, □ apparent base from image ◊ determination of base from data in Fig. 11